Spatial variations in $PM_{2.5}$ physico-chemical characteristics and associated health risk in an urban coastal city

Shruti Tripathi (shrutitripathi@iitb.ac.in)
Indian Institute of Technology Bombay
Abhishek Chakraborty
Indian Institute of Technology Bombay
Debayan Mandal
Indian Institute of Technology Bombay

Research Article

Keywords: Organic Carbon, Elemental Carbon, Organic Aerosol, Char-EC and Soot-EC, Risk assessment, Lung deposition

Posted Date: February 7th, 2023

DOI: https://doi.org/10.21203/rs.3.rs-2541578/v1

Additional Declarations: No competing interests reported.

Version of Record: A version of this preprint was published at Journal of Atmospheric Chemistry on July 3rd, 2023. See the published version at https://doi.org/10.1007/s10874-023-09448-5.

Abstract

This paper investigates the chemical composition of Particulate Matter, Organic Carbon (OC), and Elemental Carbon (EC) in residential and traffic sites in Mumbai. The average $PM_{2.5}$ and PM_{10} concentrations at the traffic site (Sakinaka) were 240 μg/m^3 and 424 μg/m^3, respectively. The observed levels of OC were 35 μg/m^3, 22 μg/m^3, and 15.5μg/m^3 at Sakinaka junction (high-density traffic), YP-Gate (low-density traffic), and Hostel Premise (Residential), respectively. The average OC/EC ratio value was high (4.5) at the residential site, indicating contributions from stationary combustion sources and secondary production of carbonaceous species to OC. The residential site has a higher percentage of low volatile OC fraction (57%) in total OC than the traffic sites. On the other hand, Sakinaka has a higher percentage of highly volatile OC fractions (36%) in total OC. The crustal-originated metals were dominating in all areas, but the concentration of metals from anthropogenic sources was highest at Sakinaka, i.e., As (381 ng/m^3), Pb (352 ng/m^3), Zn (679 ng/m^3). The K/Al, Ca/Al, Mg/Al, and Fe/Al ratios were high in all the samples compared to the crustal ratio indicating biomass burning and traffic emission sources of these metals. PM originating from traffic was more enriched with heavy metals that are toxic to human health, increasing cancer risks (CR) through inhalation. The hazard quotient was above 1 at all the locations, and CR was above $1x10^{-4,}$ causing health risks. According to the dosimetry model, more PM was deposited in the lungs of traffic location occupants through inhalation, increasing the cancerous risk.

1. Introduction

Air pollution is the leading cause of worldwide premature death. Around 7 million people die prematurely from indoor and outdoor air pollution (Im et al. 2015). Traffic and urbanization at local and regional levels affect air quality and ecosystems. In Mumbai, the emission from the traffic sector nearly doubled in the past four years, from 16% (2016) to 30.5% (2019–2020) (SAFAR 2021). The risk of cardiopulmonary death is connected with long-term exposure, while respiratory difficulties are associated with short-term exposure (WHO, 2013). The atmospheric aerosol, one of the major air pollutants, impacts human health, visibility, and climate change (Kroll and Seinfeld 2008). The metals are a significant component of atmospheric aerosols and cause various toxic effects and health risks (Rahman et al. 2019). These metals bioaccumulate and interfere with the physiological functioning of the human body (Bolognin et al. 2009). They are the primary cause of oxidative stress in the body and mitochondrial damage, leading to cardiovascular mortality and morbidity (Araujo and Nel 2009).

Inorganic and organic components are present in particulate matter or atmospheric aerosols. Organic aerosols (OA) make up a significant part of fine aerosol, up to 90% (Kanakidou et al. 2005). Oxidation, fragmentation, gas-to-particle conversion, precursor sources, and meteorology affect OA chemical composition. Also, it varies spatially and temporarily (Q. Zhang et al. 2011). Organic and elemental carbon concentrations (OC & EC) are initially determined to measure organic aerosol in PM (Turpin and Huntzicker 1995). Visibility is significantly reduced by the EC, while solar radiation is scattered by the OC

(Kirkevåg et al. 2013). In addition to reducing atmospheric visibility, this can alter the characteristics of clouds and precipitation radiation that affect global climate change (Jacobson 2016). A long-term, high-resolution dataset is required to understand EC-OC dynamics, determine their causes, and implement effective mitigation methods. As a result of incomplete combustion, EC is the most common product. On the other hand, anthropogenic or biogenic OC can be released directly into the atmosphere (primary organic carbon, POC), or oxidative species interact with organic precursors to produce less volatile products, which are then partitioned from gas to particle phase (secondary organic carbon, SOC) (Kroll and Seinfeld 2008). OC consists of hundreds of molecules with different chemical and physical properties. It is difficult to directly estimate the contributions of primary and secondary organic aerosol components by chemical analysis. A thermal optical analyzer (TOA) analyses the concentration of OC and EC based on the volatility of different organic and elemental carbon fractions in $PM_{2.5}$ (Aslam et al. 2020).

According to IQAir, India was placed 5th place in 2021 on the most polluted country's list (IQAir). The Indo-Gangetic Plain is the most polluted and studied region in India, and during winter, air quality is generally in the unhealthy to hazardous range. Compared to IGP, fewer studies were conducted in other parts of the country (Chowdhury et al. 2007; Joseph et al. 2012). The air quality in these cities falls under the unhealthy category (Aqi.in), and one of them is Mumbai, the financial capital of India, which lies in the western part of India. The particulate matter concentration (PM) was nine times higher than the WHO limit in 2021 in Mumbai (IQAir). The reported average $PM_{2.5}$ for Mumbai in winter 2021 was 80 $\mu g/m^3$ (SmartAIR), above the NAAQ annual standard (40 $\mu g/m^3$).

This study aims to examine the air quality of the metropolitan coastal city of India and the influence of air pollutants on the health of the residents. The spatial distribution of OC and EC is studied. The focus is on residential, low-density traffic, and high-density traffic sites. The particulate matter samples were collected during the day at all three locations. The impact of traffic on particulate matter concentration and composition is investigated. This study will help to investigate the effects of air pollutants on climate and human health and implement strategies for air pollution mitigation, particularly in heavy traffic-impacted megacities such as Mumbai.

2. Research Methodology

2.1 Sampling sites and sample collection

The organic carbon concentration all over India is in a higher range, even in western India (Fig. 1). In this study, November and December were covered for sampling. Measurements were performed in Mumbai, at the Indian Institute of Technology Bombay (IITB) campus, and Sakinaka, a traffic Junction (Fig. 1).

In IITB, two locations were chosen, one is close to the road (YP-Gate), and another is a residential site (Hostel Premise, HP). The sampling location at YP-Gate has modest traffic, whereas Sakinaka has significantly higher traffic volumes than YP gate (www.tomtom.com). The $PM_{2.5}$ samples were taken

using a mini volume sampler for 10 hours (9:00AM to 7:00PM) at a flow rate of 5 L per min on 47 mm quartz microfiber and Teflon (PTFE) filters. Quartz filters were heated at 600°C for 6 hours in a muffle furnace to remove organic impurities before sampling. The sampling was performed on alternate days from November to December (2021) and total 23 (15 Quartz and 8 Teflon) filters were collected at each YP-Gate and Hostel premise, whereas 16 (8 Quartz and 8 Teflon) filters were collected at Sakinaka Junction simultaneously. An optical Particle Counter (OPC) was used to capture PM size and mass distribution at each location, and sampling was done simultaneously with a mini vol sampler.

2.2 Measurement and analysis of $PM_{2.5}$ samples

The TOA from Sunset laboratory was used to measure OC and EC concentrations in $PM_{2.5}$ samples collected on quartz filters. The methodology used for analysis is based on IMPROVE (Birch 1998). The sampling analysis is divided into two phases. As a first step, OC is volatilized from the sample in a non-oxidizing environment at different temperatures (340°C, 500°C, and 615°C) for 60 seconds and 90 seconds (870°C). Second, the oven is cooled to below 500°C for 60 seconds, and helium and oxygen are introduced. The temperature gradually increases to 850°C, maintained for 45 seconds, and 900°C for 120 seconds. Four OC fractions, pyrolyzed carbon, and three EC fractions were produced on the thermograph (Jamhari et al. 2022). PM's elemental components (Si, Ti, Mn, Zn, As, and Se) were analyzed using Teflon filters by energy-dispersive X-ray fluorescence (EDXRF). A spiked quantity of element mass was used to determine element recovery efficiencies. The inorganic components of PM are analyzed by using the ion chromatography method. The samples collected on quartz filters were extracted ultrasonically for 120 minutes using 20 ml of deionized water. The insoluble matters were filtered out by using 0.22 um nylon membrane filters then the sample was analyzed in an ion chromatography system for the concentration of each cation (Na^+, K^+, NH_4^+, Ca^{2+}) and anion (Cl^-, F^-, Br^-, NO_3^-, SO_4^{2-}). The blank filters were also analyzed for blank corrections. The peak was observed against a standard solution.

2.3 Exposure Assessment

Air pollution in these areas is likely to expose residents to metals. They are classified based on age group, children (0–15) and adults (Sah et al. 2019). The risk of heavy metals in $PM_{2.5}$ is assessed based on daily chemical intake (CDI), dermal absorbed dose (DAD), and exposure concentration (EC) is calculated according to the human health evaluation manual (Part A), as well as additional guidance for assessing dermal risk (Part E) and inhalation Part F. The following were the equations and abbreviations mentioned in the supplementary document (Table SI 1):

$$CDI\,(ingest) = [(C \times IngR)/BW] \times [(EF \times ED)/AT] \times CF$$

1

$$DAD\,(dermal) = [(C \times SA \times AF \times ABS)/BW] \times [(EF \times ED)/AT] \times CF$$

2

$$EC\,(Inhalation) = (C \times ET \times EF \times ED)/AT_n$$

3

Where: C is the metal concentrations, IngR: is ingestion rate; ED: is exposure duration; EF: is exposure frequency; BW: is body weight; AT: averaging time, CF: is the conversion factor, SA: is skin surface area exposed to airborne particulates; AF: adhesion factor for airborne particles on the skin; ABS: absorption factor dermal; ET: exposure time; ATn: average time calculated by multiplying 24 by the AT.

Risks were quantified independently for non-carcinogenic and carcinogenic impacts. A hazard quotient was used to assess the non-carcinogenic danger (HQ) and cancer risk (CR) for carcinogenic effects. The following equations were used to evaluate the HQ and CR of heavy metals in $PM_{2.5}$ via ingestion, dermal contact, and inhalation.

$$HQ = \frac{CDI}{RfDo} = \frac{DAD}{(RfDo \times GIABS)} = \frac{EC}{(RfCi \times 1000 \mu g m g^{-1})}$$

4

$$CR = CDI \times SFo = DAD \times \left(\frac{SFo}{GIABS}\right) = IUR \times EC$$

5

Sfo, RfDo, RfC, GIABS, and IUR are taken from US environmental protection agency screening level report (USEPA 2011). The RfDo is oral reference dose, RfCi is inhalation reference concentration, Sfo is oral slope factor, GIABS is gastrointestinal absorption factor, and IUR is inhalation unit risk.

2.4 Human Respiratory Tract Deposition Model

The multiple path particle dosimetry models (MPPD, v3.04) calculate particulate matter's deposition fraction at different parts of the human lungs. This model can calculate regional and overall PM deposition and clearance from the other respiratory system parts. The input parameters of this model are 1. airway morphology, 2. particle properties, and 3. exposure scenarios. The detail of the model description can be found in various studies (Lv et al. 2021; Zwozdziak et al. 2017). The human airway morphology differs for adults and children, so an age-specific 5-lobe model was used in this study (Menache 1995). The model was run for two scenarios, i.e., adults and children.

3. Result And Discussion

3.1 Meteorological Parameters

The climate of Mumbai is wet & dry tropical and highly influenced by the Asian monsoon. The distinction between summer and winter is not significant. During sampling time, the average planetary boundary layer height (PBLH) was 772m during the day and 661m at night (Merra data NASA). The average

temperature was between 25–32 ^{o}C, and relative humidity was 40–50% (CPCB.nic.in). The wind rose for HP, and the YP-Gate site was obtained from the MPCB monitoring station (Powai), depicting that the wind had blown from YP-Gate to HP (Fig. SI 1). The nearest CPCB station for Sakinaka is 2km from the sampling site, so it would not be a true representation of wind patterns at the Sakinaka site. With the Hybrid Single-Particle Lagrangian Integrated Trajectory model (HYSPLIT), backward trajectories of air masses arriving at a specific location can be generated. This model indicates that in Mumbai city, air came from the inland area during the sampling (Fig. SI 2).

3.2 PM Size and Mass Distribution

The PM_{10}, $PM_{2.5,}$ and PM_1 concentrations at all three locations are mentioned in Table SI 2, along with some other global studies. PM mass and number concentration data were collected through OPC that was collocated with a Mini-vol sampler at all three locations. The concentration of particulate matter is an average of eight hours of sampling duration (09:00 AM to 05:00 PM). The highest PM concentrations are reported at Sakinaka and the lowest at HP. PM deposited on the lung surface can induce tissue damage, corrode the alveolar wall, and impair the lung (Douglas et al. 2018; Xing et al. 2019). The $PM_1/PM_{2.5}$ and $PM_{2.5}/PM_{10}$ ratios are higher at HP (0.72 & 0.78), followed by YP (0.62 & 0.78) and Sakinaka (0.49 & 0.56), denoting the enhancement of fine mode particles in HP and YP. The lower ratio in Sakinaka suggests the dominance of coarse mode particles (Chauhan and Singh 2021). The coarse-size particle sources were road abrasion, brake, and tire wear (Kumar et al. 2018). Furthermore, commuters were more at the sampling location since the Sakinaka metro station was nearby, so coarse particles remained resuspended due to various movements

The lognormal mass size distribution in the morning, fine PM mass distribution peak (9 AM to 11 AM) was highest compared to other times of the day at Sakinaka (Fig. 2). Also, the maximum peak was observed at 0.25 µm and 0.9 µm. The YP-Gate is close to the traffic site, so the particles were highest in the morning, whereas at HP (residential area), these were highest in the noon hours. The PM mass size distribution peak was observed at 0.4 µm in HP and 0.33 µm in YP-Gate. The normalized number concentration also shows that the same peak was observed around 0.4 µm in HP (Fig. SI 3). The distribution pattern and particulate matter peak at Sakinaka differed from the other two locations. These distributions signify the emissions from the vehicles during morning rush hours, and the peak denotes the highest contribution of specific-size particles.

3.3 Carbonaceous aerosol distribution and levels

Due to major anthropogenic sources and secondary production via chemical processes in the atmosphere, OC concentrations were higher than EC at all sampling sites. Mean EC levels were 3.5 µg/m^3, 8.5 µg/m^3, and 13 µg/m^3 for HP, YP-Gate, and Sakinaka sites, respectively (Fig. 3a). The OC concentration was 15.5 µg/m^3, 22 µg/m^3, and 35 µg/m^3 respectively (Fig. 3b). Among these three sites, average OC and EC concentrations were highest at Sakinaka, attributable to the mixed contribution from high traffic flows. Due to its downwind location (Fig. SI 1) from anthropogenic emission sources, HP had the lowest concentrations of OC and EC. The study conducted in the year 2007 reported OC

concentrations were 28 μg/m^3 and 31 μg/m^3, whereas EC concentrations were 9 μg/m^3 and 7 μg/m^3 (Joseph et al. 2012). Compared to previous studies, this study's OC & EC concentration is comparable and even slightly higher. The average values for the OC/EC ratio were 4.5, 2.5, and 2.8 at HP, YP-Gate, and Sakinaka sites, respectively; OC/EC ratios greater than 2 have been considered an indicator of SOA formation due to contributions to OC from both combustion sources and secondary formation of carbonaceous materials (Hildemann, Markowski, and Cass 1991). High OC by EC ratio in $PM_{2.5}$ denotes dominance of secondary organics fraction in fine particulate matter. PM composition in Sakinaka may be receiving more contributions from resuspended road dust due to higher traffic volumes.

The organic aerosol (OA) is calculated by multiplying OC by 2 (for an urban area), as many Indian studies indicated the same based on online and offline organic aerosol characterization (Chakraborty, Tripathi, and Gupta 2017). Total carbonaceous aerosol (TCA) is estimated by the sum of EC and OA [TCA = 2 × OC (or OA) + EC] (Rengarajan, Sarin, and Sudheer 2007; Turpin and Huntzicker 1995). The OA contribution to $PM_{2.5}$ (29.6%) is more at Sakinaka than at the other two sites. The EC values were also higher at Sakinaka due to primary vehicular emissions. The mean TCA concentrations were 34.5, 52.5, and 83 μg/m^3 at HP, YP-Gate, and Sakinaka, respectively. Anthropogenic emissions of carbonaceous aerosols and unfavorable meteorological conditions may contribute to the higher TCA contribution, such as low wind speed, low mixing height, frequent inversions, etc., resulting in pollution stagnation (Pachauri et al. 2013). High automobile emissions may be responsible for higher TCA levels in traffic areas. While at the residential site, carbonaceous aerosols were primarily generated by widespread biomass burning (Pachauri et al. 2013).

The chemical characterization of $PM_{2.5}$ samples at all three locations has shown that anions at HP have the highest percentage of $PM_{2.5}$ than the other two locations (Fig. 4). The percentage of cations and anions is higher in the coastal region $PM_{2.5}$ in comparison to the inland region (Table SI 3). The transportation sector is the major source of nitrate and residential activities for sulfate (H. Zhang et al. 2012). The higher fractions of Na and Cl in all the sites might indicate sea salts.

3.4 The volatility of Organic Aerosol

The OC fraction is analyzed by a TOA (Section 2.2) based on its volatility. Four temperature-resolved OC fractions (OC1, OC2, OC3, and OC4) are obtained, with OC1 to OC4 having decreasing volatility. This atmospheric OC property (volatility) has been utilized to distinguish between distinct sources of PM, total OC, and OC volatility fractions in various metropolitan settings (Soleimanian et al. 2019). The OC1 exists mostly in the vapor phase (Liu et al. 2006). The OC2 and OC3 fractions in the particulate matter come from the gasoline and diesel factor (Kim, Hopke, and Edgerton 2004). The PMF study showed that OC4 is mainly associated with secondary coal sources that have traveled farther from local traffic emitted OC (Lee 2003). The OC and EC levels vary at all three locations (Table SI 4). The concentration of OC1 is nil in all three areas, and the other fractions of OCs (OC2 to OC4) were highest at Sakinaka compared to YP-Gate and HP. OC2 and OC3 concentrations at Sakinaka were way higher than OC4 concentrations. Sakinaka is a traffic site with very high and continuous traffic volumes, so OC2 and OC3 values were

higher in Sakinaka. Though YP-Gate is also close to the traffic location, the concentration of OC2 and OC3 was less than in Sakinaka. The OC4 concentration at the HP was slightly higher than YP-Gate. That denotes more dominance of secondary PM fraction at the HP. Contribution of low volatile organic fraction (OC4) fraction to total OC was 0.21, 0.16, and 0.19 at HP, YP-Gate, and Sakinaka, respectively. The higher volatile OC fraction (OC2 and OC3) in total OC was 0.66, 0.56, and 0.79 at the HP, YP-Gate, and Sakinaka. The HP had a higher fraction of low volatile OC than the other two traffic sites, indicating more dominance of secondary organics. In contrast, Sakinaka has a more high-volatile OC fraction in total OC, indicating more primary organics emissions during sampling. YP-Gate's mean OC value is between the Sakinaka and HP's values in both scenarios denoting a mixture of traffic emissions and secondary formation.

3.5 Char-EC and Soot-EC

Emissions of EC come mainly from combustion emissions, which are primarily anthropogenic (tire exhaust and fossil fuel and biomass combustion) and divided into char and soot. Char and soot are separated by size and range from heavily condensed refractory submicron soot particles to large pieces of lightly charred material (Han et al. 2007; Zhan et al. 2008). Char-EC/Soot-EC ratios have been used to identify sources (Han et al. 2009). Char is produced by burning solid residues, whereas soot is produced by incomplete combustion. Depending on the type of combustion, their ratios will vary between different source categories (Han et al. 2010). Char-EC is the difference between EC1 and OP, and soot-EC is the sum of EC2 and EC3. Residential cooking produces char-EC/soot-EC, generally within the range of 2.0 to 6.0 (Chow et al. 2004). Higher char/soot ratios indicate the major influence of biomass combustion and coal combustion, whereas lower char/soot ratios indicate the major impact of vehicular exhaust (Wang et al., 2019). The spatial distribution of the ratio is shown in table SI 5. Additionally, the relationship between OC and EC can be used to assess the origin of carbonaceous aerosols (Cao et al. 2006). OC/EC for biomass combustion was 6.6, and 0.7 for motor vehicle emissions (Saarikoski et al. 2008). A ratio of OC/EC above 5 can indicate increased biomass burning, while OC/EC ratios below 2 may indicate fossil fuel combustion or motor vehicle emissions (Rastogi et al. 2016). As discussed in section 3.3, OC/EC ratios range from 2.8 to 4.5, indicating diverse emissions sources from biomass burning and vehicular emissions (Table SI 5).

Char-EC and Soot-EC have the highest correlation at Sakinaka, with an R^2 value of 0.8 ($p < 0.05$) (Fig. SI 4). Char-EC and Soot-EC are likely to originate from fuel combustion in vehicular engines. On the other hand, YP-Gate and HP have positive but relatively lower R^2 values, around 0.6. This indicates different sources and formation mechanisms, such as char formed from combustion residues and soot formed by gas conversion (Zhan et al. 2019). $PM_{2.5}$ char correlated more strongly with OC and EC than soot. The formation mechanism of Char-EC explains the strong correlation. It is formed by incomplete combustion and soot to particle transformation by condensation.

3.6 Metal concentration and emission factor

High airborne trace element concentrations can negatively impact air quality and human health (Xia and Gao 2011). As metals derived from pollution are frequently concentrated on small particles, they may stay suspended in the air for extended periods and effectively enter the human lungs. Therefore, the particulate toxicity of fine aerosol particles may be influenced by trace metals (Gao et al. 2002). The crustal-originated metal concentrations, i.e., Al, Ca, and Fe, are higher in HP. In contrast, industrial and traffic-related metals are more elevated in YP-Gate and Sakinaka, i.e., Ba, Cu, Cr, Mn, Pb, Zn, and As (Table SI 6). After oxygen and silicon, Al and Fe are the third and fourth most abundant metals in the Earth's crust, with a typical Fe/Al ratio of approximately 0.44 for the upper continental crust (Rudnick 2000). In this study, the ratios are 1.08, 1.48, and 1.56 at HP, YP-Gate, and Sakinaka, respectively, which is more than the crustal ratio and indicates anthropogenic contamination of the dust at these locations. Near the traffic junction, the highest ratio indicates some traffic originated Fe. The ratio of Fe/Al in soil resuspension is around ~ 0.9 (Engelbrecht et al. 2016), close to the ratio obtained for HP. Cu concentrations in all three locations were low, so the ratios of Cu/Zn and Cu/Pb are also low compared to road dust (0.17 and 0.96, respectively) (Shen et al. 2016) (Fig. 5). The Ca/Al, and Mg/Al ratios are higher than the crustal ratio, i.e., 0.37 and 0.17, respectively (Mclennan 2001). The K/Al ratio was significantly higher than upper continental crustal values (0.35) at HP (4.9), followed by YP (4.5) and Sakinaka (1.7). Potassium is generally an indicator of biomass burning emissions.

The enrichment factor (EF) is calculated to study the impact of anthropogenic emissions on these metals in $PM_{2.5}$. The EF is also widely used for the source identification of chemical constituents of $PM_{2.5}$ samples. It is calculated by comparing elements' concentration in the ambient aerosol to their concentration present in the Earth's crust. The element's crustal concentration has been taken from Hans Wedepohl 1995. The EF is calculated using Eq. 3 by taking aluminum (Al) as a reference element for a geogenic source (Mehra et al. 2020).

$$Enrichment Factor = \frac{\left(\frac{Element}{Referenceelement}\right)_{sample}}{\left(\frac{Element}{Referenceelement}\right)_{crustal}}$$

6

All the value of EF above 10 is plotted in Fig. 6. The degree of Lead enrichment (Pb) is high in all the locations, i.e., 1707.63 (Sakinaka), 1676.78 (YP-Gate), and 391.93 (HP), and for Arsenic (As) is 3100, 3593.8 and 8490 respectively. Zinc (Zn), Copper (Cu), and Bromine (Br) have high EF values, in between the range of 10-1000. The sulfur enrichment is varied in Sakinaka > YP-Gate > HP decreasing manner. Cu is also a tracer of traffic emissions (Dongarrà et al. 2007). Sources of sulfur are fossil fuel and biomass-burning emissions (Reddy and Venkataraman 2002). Even though the EF values of metals are higher at YP and Sakinaka, the percentage of metal concentration in total $PM_{2.5}$ is slightly higher in HP samples. The crustal metals contribute more to $PM_{2.5}$ than the anthropogenic ones at HP, whereas traffic sites have more anthropogenically emitted metals in $PM_{2.5}$. EF value for Cd is reported in the range of 1000–15000 in various studies at urban sites (Jack et al. 2020; Li et al. 2016; Lin and Wang 2020). The toxic heavy metals are more enriched in traffic samples, i.e., As, Cd, and Pb. High enrichment of these metals

suggests the dominant source is anthropogenic activities, like traffic emissions and biomass burning. Long-term exposure to arsenic and Cd can cause cancer of the bladder and lungs, whereas lead exposure could cause kidney and brain damage (WHO 2018 and NIOSH).

3.8 Exposure assessment of heavy metals and lung deposition

Daily exposure to air pollutants has serious health problems. Some metals in the particulate matter have carcinogenic risk (CR) that increases the toxicity of aerosols. The acceptable limit for total CR is from 1×10^{-6} to 1×10^{-4}. The non-carcinogenic metals are still hazardous to human health and are assessed under Hazard Quotient (HQ). The Hazard Index (HI) is the sum of HQ of all the non-carcinogenic metals (Sui et al. 2020). If the HI is below 1, it does not possess any harmful effects but has serious health issues if it is above 1. The hazardous and toxic metals are studied in this study for their carcinogenic and non-carcinogenic effects on Adults' and Children's health. The hazard risk and cancer risk for inhalation, digestion, and dermal exposure are calculated (section 2.3), and the result is summarised in Tables 1 and SI 7 & 8.

The HI value for children's exposure assessment for inhalation is greater than 1 at all locations. The CR value for inhalation is higher than 1×10^{-4} at all three locations. Sakinaka is a congested area in terms of traffic and various shops (DriveU Blog). The nearest metro station to the sampling site also adds extra crowding during office morning/evening hours. Due to this situation, health is more at risk from exposure. Cd, As, and Cr metals are the main contributors to CR and HI. The toxicity effect of metals through dermal and ingestion is under the safe limit at all three locations (Table SI 7 & 8). These findings indicate elemental exposure from dermal and ingestion will not result in non-carcinogenic and carcinogenic adverse effects on adults and children. Whereas through inhalation, $PM_{2.5}$ causes health risks in both adults and children.

Table 1
Hazard and cancer risk index for inhalation at all three locations for adults and Children

Hazard Index for inhalation						
Metals	**Sakinaka**		**YP-Gate**		**HP**	
	HQ (Adult)	**HQ (Children)**	**HQ (Adult)**	**HQ (Children)**	**HQ (Adult)**	**HQ (Children)**
Cr	2.3	2.3	0.033	0.033	0.03	0.03
Mn	.16	.16	0.21	0.21	0.2	0.2
Pb	.38	.38	0.14	0.14	0.06	0.06
S	2.1	2.1	3.2	3.2	3	3
Ti	0.3	0.3	0.13	0.13	0.06	0.06
Cd	4.9	4.9	0.16	0.16	0.43	0.43
As	0.5	0.5	0.82	0.82	0.6	0.6
HI	**11**	**11**	**4.7**	**4.7**	**4.4**	**4.4**
Cancer Risk for inhalation						
Metals	**Sakinaka**		**YP-Gate**		**HP**	
	CR (Adult)	**CR (Children)**	**CR (Adult)**	**CR (Children)**	**CR (Adult)**	**CR (Children)**
Cr	6.6E-07	1.7E-07	9.5E-05	2.4E-05	9.0E-05	2.2E-05
Pb	5.1E-07	1.3E-07	1.9E-03	4.6E-04	8.5E-04	2.1E-04
Cd	3.0E-06	7.6E-07	1.0E-06	2.5E-07	2.6E-06	6.6E-07
As	7.3E-05	1.8E-05	1.2E-05	3.6E-06	9.7E-06	2.4E-06
Total CR	**1.2E-02**	**2.9E-03**	**2.0E-03**	**4.9E-04**	**8.9E-04**	**2.3E-04**

The MPPD model is used to estimate PM deposition through inhalation. The count median diameter and the geometric standard deviation are required in this model, along with PM concentration as model input (Manojkumar et al., 2019). The calculated deposited mass (µg) of PM in the lung is represented in fig. SI 5 for adults (Age 21) and children (Age 14). The mass deposition in adults is higher than in children. The highest deposition is observed in residents of the Sakinaka site, followed by YP-Gate and HP. Sakinaka residents are more prone to health risks from PM than the other two sites. Among all study sites, depositions of $PM_{2.5}$ were highest in the head region (42%), whereas PM_1 depositions were highest in the pulmonary (59%). Ultrafine particles should be included in the current air-quality index since they are most prevalent in the lungs.

4. Conclusions

The impact of traffic on overall air quality and the properties of OC and EC in urban traffic and residential areas in Mumbai were investigated in $PM_{2.5}$ samples. EC concentrations were highest at Sakinaka and lowest at HP due to its location upwind of anthropogenic emission sources (YP-Gate). On the other hand, the OC/EC ratio was highest at HP due to contributions to OC from stationary combustion sources and secondary production processes. The TCA percentage in $PM_{2.5}$ ranges from 33–55%, demonstrating that carbonaceous species are abundant in fine particles at all three sampling sites. The OC fractions are also differentiated based on volatility, and the HP has a high percentage of low-volatile OC fractions, while Sakinaka has high-volatile OC fractions. The ratio of OC/EC and percentage of OC fractions in total OC show the diverse nature of $PM_{2.5}$ samples. Sakinaka is traffic influenced, and the HP is a residential site, but YP-Gate is low-density traffic with a residential area. Char-EC and Soot-EC ratios indicate the same; the HP ratio implies biomass-burning sources, while Sakinaka and YP-Gate suggest vehicular emissions and biofuel burning. The correlation between Char-EC and Soot-EC is highest at Sakinaka, denoting both char and soot have the same origin, i.e., traffic emission. The correlation at the other two sites is low compared to the previous site, signifying diverse sources.

The organic and inorganic compounds were high in Sakinaka samples because of the high emissions at this site. YP-Gate has lower emissions than Sakinaka, followed by HP. The crustal-originated metal concentrations, i.e., Al, Ca, and Fe, are higher in HP. In contrast, industrial and traffic-related metals are higher in YP-Gate and Sakinaka, i.e., Ba, Cu, Cr, Mn, Pb, Zn, and As. The ratio of these metals also suggested anthropogenic source contribution to the aerosols, i.e., traffic and biomass burning emissions. The enrichment factor of these metals is way higher in Sakinaka samples compared to HP and YP-Gate. The assessment of the cancer risk from these heavy metals has shown a risk of cancer in adults and children of all these three locations' residents through chronic daily intake via inhalation of pollutants in their lifetime. The lung deposition model also showed that PM deposition is higher in residents of Sakinaka. So, in conclusion, Sakinaka is at higher risk for the health effects of emissions of air pollutants. YP-Gate has also shown the impact of traffic emissions on air quality and influences the HP pollutants concentration. The findings of this study clearly show that even in a coastal city like Mumbai, air quality issues are severe, and the exposed population is at risk of developing health issues. Given the tremendous heterogeneity observed in PM levels and composition at different locations, policymakers should develop area-specific pollution mitigation measures to improve the city's air quality.

Declarations

Funding

The authors declare that no funds, grants, or other support were received during the preparation of this manuscript.

Competing Interests

The authors have no relevant financial or non-financial interests to disclose.

Author Contributions

Shruti Tripathi-Conceptualization; Data curation; Formal analysis; Methodology; and Writing original draft. Abhishek Chakraborty- Supervision, reviewed and edited. Debayan Mandal- Review and editing.

Data Availability

The datasets generated during and analyzed during the current study are not publicly available but are available from the corresponding author at a reasonable request.

Ethics approval

Not applicable

Consent to participate

Not applicable

Consent to publish

Not applicable

References

1. Araujo, Jesus A, and Andre E Nel. 2009. “Particle and Fibre Toxicology Particulate Matter and Atherosclerosis: Role of Particle Size, Composition and Oxidative Stress.” http://www.particleandfibretoxicology.com/content/6/1/24.
2. Aslam, Afifa et al. 2020. “Pollution Characteristics of Particulate Matter (PM2.5 and PM10) and Constituent Carbonaceous Aerosols in a South Asian Future Megacity.” *Applied Sciences (Switzerland)* 10(24): 1–17.
3. Birch, M. Eileen. 1998. “Analysis of Carbonaceous Aerosols: Interlaboratory Comparison.” *Analyst* 123(5): 851–57.
4. Bolognin, Silvia et al. 2009. “Metal Ion Physiopathology in Neurodegenerative Disorders.”
5. Cao, J.J. et al. 2006. “Characterization of Roadside Fine Particulate Carbon and Its Eight Fractions in Hong Kong.” *Aerosol and Air Quality Research* 6(2): 106–22.
6. Chakraborty, Abhishek, S N Tripathi, and Tarun Gupta. 2017. “Effects of Organic Aerosol Loading and Fog Processing on Organic Aerosol Volatility.” *Journal of Aerosol Science* 105(November 2016): 73–83. http://dx.doi.org/10.1016/j.jaerosci.2016.11.015.
7. Chauhan, Akshansha, and Ramesh P. Singh. 2021. “Effect of Lockdown on Hcho and Trace Gases over India during March 2020.” *Aerosol and Air Quality Research* 21(4): 1–19.

8. Chow, Judith C. et al. 2004. “Source Profiles for Industrial, Mobile, and Area Sources in the Big Bend Regional Aerosol Visibility and Observational Study.” *Chemosphere* 54(2): 185–208.
9. Chowdhury, Zohir et al. 2007. “Speciation of Ambient Fine Organic Carbon Particles and Source Apportionment of PM2.5 in Indian Cities.” *Journal of Geophysical Research Atmospheres* 112(15): 1–14.
10. Dongarrà, G., E. Manno, D. Varrica, and M. Vultaggio. 2007. “Mass Levels, Crustal Component and Trace Elements in PM10 in Palermo, Italy.” *Atmospheric Environment* 41(36): 7977–86.
11. Douglas, Philippa et al. 2018. “A Systematic Review of the Public Health Risks of Bioaerosols from Intensive Farming.” *International Journal of Hygiene and Environmental Health* 221(2): 134–73.
12. Engelbrecht, Johann P. et al. 2016. “Technical Note: Mineralogical, Chemical, Morphological, and Optical Interrelationships of Mineral Dust Resuspensions.” *Atmospheric Chemistry and Physics* 16(17): 10809–30. https://acp.copernicus.org/articles/16/10809/2016/ (September 14, 2022).
13. Gao, Y. et al. 2002. “Characterization of Atmospheric Trace Elements on PM2.5 Particulate Matter over the New York–New Jersey Harbor Estuary.” *Atmospheric Environment* 36(6): 1077–86.
14. Han, Y. M. et al. 2009. “Elemental Carbon in Urban Soils and Road Dusts in Xi’an, China and Its Implication for Air Pollution.” *Atmospheric Environment* 43(15): 2464–70.
15. Han, Y. M. et al.. 2010. “Different Characteristics of Char and Soot in the Atmosphere and Their Ratio as an Indicator for Source Identification in Xi’an, China.” *Atmospheric Chemistry and Physics* 10(2): 595–607. https://acp.copernicus.org/articles/10/595/2010/ (September 14, 2022).
16. Han, Yongming et al. 2007. “Evaluation of the Thermal/Optical Reflectance Method for Discrimination between Char- and Soot-EC.” *Chemosphere* 69(4): 569–74.
17. Hans Wedepohl, K. 1995. “The Composition of the Continental Crust.” *Geochimica et Cosmochimica Acta* 59(7): 1217–32.
18. Hildemann, Lynn M, Gregory R Markowski, and Glen R Cass. 1991. 25 In Onondaga County Monitoring Program Annual Report *Heavy Metal Distribution in Particles from the Flocculent Sediments of Onondaga Lake*. Wiley and Sons. https://pubs.acs.org/sharingguidelines.
19. Im, Ulas et al. 2015. “Evaluation of Operational Online-Coupled Regional Air Quality Models over Europe and North America in the Context of AQMEII Phase 2. Part II: Particulate Matter.” *Atmospheric Environment* 115: 421–41.
20. Jack, Shaofeng Sui et al. “Pollution Characteristics and Chronic Health Risk Assessment of Metals and Metalloids in Ambient PM 2.5 in Licheng District, Jinan, China.” *Environmental Geochemistry and Health* 42. https://doi.org/10.1007/s10653-019-00448-7.
21. Jacobson, Mark Z. 2016. “Strong Radiative Heating Due to Mixing State of Black Carbon in Atmospheric Aerosol . Mixing State of Black Carbon in Atmospheric Aerosols.” 409(January 2001): 695–97.
22. Jamhari, Anas Ahmad et al. 2022. “Seasonal Variation and Size Distribution of Inorganic and Carbonaceous Components, Source Identification of Size-Fractioned Urban Air Particles in Kuala Lumpur, Malaysia.” *Chemosphere* 287: 132309.

23. Joseph, Abba Elizabeth, Seema Unnikrishnan, and Rakesh Kumar. 2012. “Chemical Characterization and Mass Closure of Fine Aerosol for Different Land Use Patterns in Mumbai City.” *Aerosol and Air Quality Research* 12(1): 61–72.
24. Kanakidou, M et al. 2005. “And Physics Organic Aerosol and Global Climate Modelling : A Review.” : 1053–1123.
25. Kim, Eugene, Philip K. Hopke, and Eric S. Edgerton. 2004. “Improving Source Identification of Atlanta Aerosol Using Temperature Resolved Carbon Fractions in Positive Matrix Factorization.” *Atmospheric Environment* 38(20): 3349–62.
26. Kirkevåg, A. et al. 2013. “Aerosol–Climate Interactions in the Norwegian Earth System Model – NorESM1-M.” *Geoscientific Model Development* 6(1): 207–44. https://gmd.copernicus.org/articles/6/207/2013/ (November 8, 2022).
27. Kroll, Jesse H., and John H. Seinfeld. 2008. “Chemistry of Secondary Organic Aerosol: Formation and Evolution of Low-Volatility Organics in the Atmosphere.” *Atmospheric Environment* 42(16): 3593–3624.
28. Kumar, Sushil, Supriya Nath, Manpreet Singh Bhatti, and Sudesh Yadav. 2018. “Chemical Characteristics of Fine and Coarse Particles during Wintertime over Two Urban Cities in North India.” *Aerosol and Air Quality Research* 18(7): 1573–90.
29. Li, Huiming et al. 2016. “Chemical Characterization and Source Apportionment of PM2.5 Aerosols in a Megacity of Southeast China.” *Atmospheric Research* 181: 288–99.
30. Lin, Yifan, and Jing Wang. “Concentrations, Enrichment, and Sources of Metals in PM 2.5 in Beijing during Winter.” https://doi.org/10.1007/s11869-019-00763-z.
31. Lv, Huitao et al. 2021. “Assessment of Pedestrian Exposure and Deposition of PM10, PM2.5 and Ultrafine Particles at an Urban Roadside: A Case Study of Xi’an, China.” *Atmospheric Pollution Research* 12(4): 112–21.
32. Mclennan, Scott M. 2001. *Relationships between the Trace Element Composition of Sedimentary Rocks and Upper Continental Crust*.
33. Mehra, Manisha, Felix Zirzow, Kirpa Ram, and Stefan Norra. 2020. “Geochemistry of PM2.5 Aerosols at an Urban Site, Varanasi, in the Eastern Indo-Gangetic Plain during Pre-Monsoon Season.” *Atmospheric Research* 234: 104734.
34. MENACHE, M. 1995. “Particle Inhalability Curves for Humans and Small Laboratory Animals.” *The Annals of Occupational Hygiene* 39(3): 317–28.
35. Pachauri, Tripti et al. 2013. “Characteristics and Sources of Carbonaceous Aerosols in PM2.5 during Wintertime in Agra, India.” *Aerosol and Air Quality Research* 13(3): 977–91.
36. Rahman, Zeeshanur, Ved Pal Singh, Z Rahman, and V P Singh. “The Relative Impact of Toxic Heavy Metals (THMs) (Arsenic (As), Cadmium (Cd), Chromium (Cr)(VI), Mercury (Hg), and Lead (Pb)) on the Total Environment: An Overview.” https://doi.org/10.1007/s10661-019-7528-7.
37. Rastogi, N., A. Singh, M. M. Sarin, and D. Singh. 2016. “Temporal Variability of Primary and Secondary Aerosols over Northern India: Impact of Biomass Burning Emissions.” *Atmospheric*

Environment 125: 396–403. http://dx.doi.org/10.1016/j.atmosenv.2015.06.010.

38. Reddy, M. Shekar, and Chandra Venkataraman. 2002. “Inventory of Aerosol and Sulphur Dioxide Emissions from India. Part II—Biomass Combustion.” *Atmospheric Environment* 36(4): 699–712.
39. Rengarajan, R., M. M. Sarin, and A. K. Sudheer. 2007. “Carbonaceous and Inorganic Species in Atmospheric Aerosols during Wintertime over Urban and High-Altitude Sites in North India.” *Journal of Geophysical Research Atmospheres* 112(21): 1–16.
40. Rudnick, Roberta L. 2000. “Rutile-Bearing Refractory Eclogites: Missing Link between Continents and Depleted Mantle.” *Science* 287(5451): 278–81.
41. Saarikoski, S. et al. 2008. “Sources of Organic Carbon in Fine Particulate Matter in Northern European Urban Air.” *Atmospheric Chemistry and Physics* 8(20): 6281–95.
42. Sah, Dinesh, Puneet Kumar Verma, Maharaj Kumari Kandikonda, and Anita Lakhani. 2019. “Pollution Characteristics, Human Health Risk through Multiple Exposure Pathways, and Source Apportionment of Heavy Metals in PM10 at Indo-Gangetic Site.” *Urban Climate* 27: 149–62.
43. Shen, Zhenxing et al. 2016. “Chemical Profiles of Urban Fugitive Dust PM2.5 Samples in Northern Chinese Cities.” *Science of The Total Environment* 569–570: 619–26.
44. Soleimanian, Ehsan et al. 2019. “Spatial Trends and Sources of PM2.5 Organic Carbon Volatility Fractions (OCx) across the Los Angeles Basin.” *Atmospheric Environment* 209: 201–11.
45. Sui, Shaofeng et al. 2020. “Pollution Characteristics and Chronic Health Risk Assessment of Metals and Metalloids in Ambient PM2.5 in Licheng District, Jinan, China.” *Environmental Geochemistry and Health* 42(7): 1803–15. https://doi.org/10.1007/s10653-019-00448-7.
46. Turpin, Barbara J., and James J. Huntzicker. 1995. “Identification of Secondary Organic Aerosol Episodes and Quantitation of Primary and Secondary Organic Aerosol Concentrations during SCAQS.” *Atmospheric Environment* 29(23): 3527–44.
47. Xia, Lili, and Yuan Gao. 2011. “Characterization of Trace Elements in PM2.5 Aerosols in the Vicinity of Highways in Northeast New Jersey in the U.S. East Coast.” *Atmospheric Pollution Research* 2(1): 34–44. http://dx.doi.org/10.5094/APR.2011.005.
48. Xing, Weiqin et al. 2019. “Inhalation Bioaccessibility of Cd, Cu, Pb and Zn and Speciation of Pb in Particulate Matter Fractions from Areas with Different Pollution Characteristics in Henan Province, China.” *Ecotoxicology and Environmental Safety* 175: 192–200.
49. Zhan, Changlin et al. 2019. “Characterization of Carbonaceous Fractions in PM2.5 and PM10 over a Typical Industrial City in Central China.” *Environmental Science and Pollution Research* 26(17): 16855–67.
50. Zhang, Hongliang et al. 2012. “Source Apportionment of PM2.5 Nitrate and Sulfate in China Using a Source-Oriented Chemical Transport Model.” *Atmospheric Environment* 62: 228–42.
51. Zhang, Qi et al. 2011. “Understanding Atmospheric Organic Aerosols via Factor Analysis of Aerosol Mass Spectrometry: A Review.” *Analytical and Bioanalytical Chemistry* 401(10): 3045–67.

52. Zwozdziak, Anna et al. 2017. “Implications of the Aerosol Size Distribution Modal Structure of Trace and Major Elements on Human Exposure, Inhaled Dose and Relevance to the PM2.5 and PM10 Metrics in a European Pollution Hotspot Urban Area.” *Journal of Aerosol Science* 103: 38–52.

Web References

1. System of Air Quality and Weather Forecasting And Research (SAFAR) http://safar.tropmet.res.in/ (Accessed on 30-05-2022)
2. WHO Health Report https://apps.who.int/iris/handle/10665/107332 (Accessed on 10-04-2022)
3. AQI.in https://www.aqi.in/world-most-polluted-cities (Accessed on 10-04-2022)
4. IQAir https://www.iqair.com/in-en/ (Accessed on 10-04-2022)
5. SmartAIR https://smartairfilters.com/en/blog/mumbai-air-quality-exceeds-8-times-who-limit-in-2021/ (Accessed on 10-04-2022)
6. Tomtom traffic index www.tomtom.com (Accessed on 01-11-2021)
7. USEPA, D. (1989). Risk assessment guidance for superfund. *Human Health Evaluation Manual Part A* (Accessed on 15-04-2022)
8. USEPA, E. (2004). Users' Guide and Background Technical Document for USEPA Region 9's Preliminary Remediation Goals (PRG) Table (Accessed on 15-04-2022)
9. Merra reanalysis data https://gmao.gsfc.nasa.gov/reanalysis/MERRA-2/ (Accessed on 15-06-2022)
10. Multiple-Path Particle Dosimetry Model (MPPD) https://www.ara.com/mppd/ (Accessed on 20-08-2022)
11. Central Pollution Control Board https://www.cpcb.nic.in (Accessed on 20-04-2022)
12. Air resource laboratory-Hysplit https://www.ready.noaa.gov/HYSPLIT.php (Accessed on 18-07-2022)
13. deadliest traffic junctions in Mumbai https://blog.driveu.in/5-deadliest-traffic-junctions-in-mumbai-85e66c4b0b3b (Accessed on 01-10-2021)

Figures

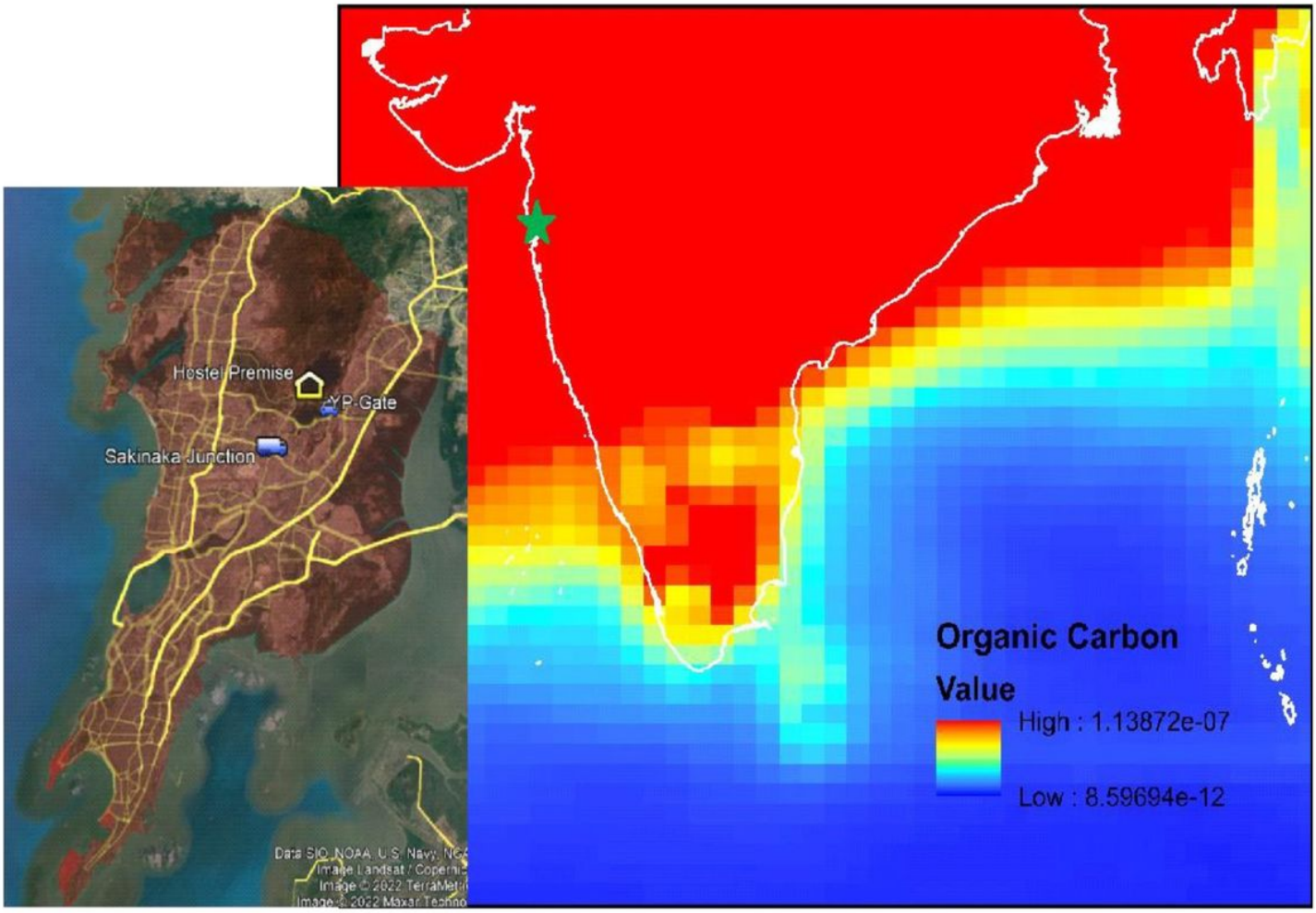

Figure 1

Study location according to emissions sources, Hostel Premise, YP-Gate, and Sakinaka-Junction in Mumbai (Source: Google Earth Pro and MERRA reanalysis data Giovanni and unit of organic carbon is kg/m^3)

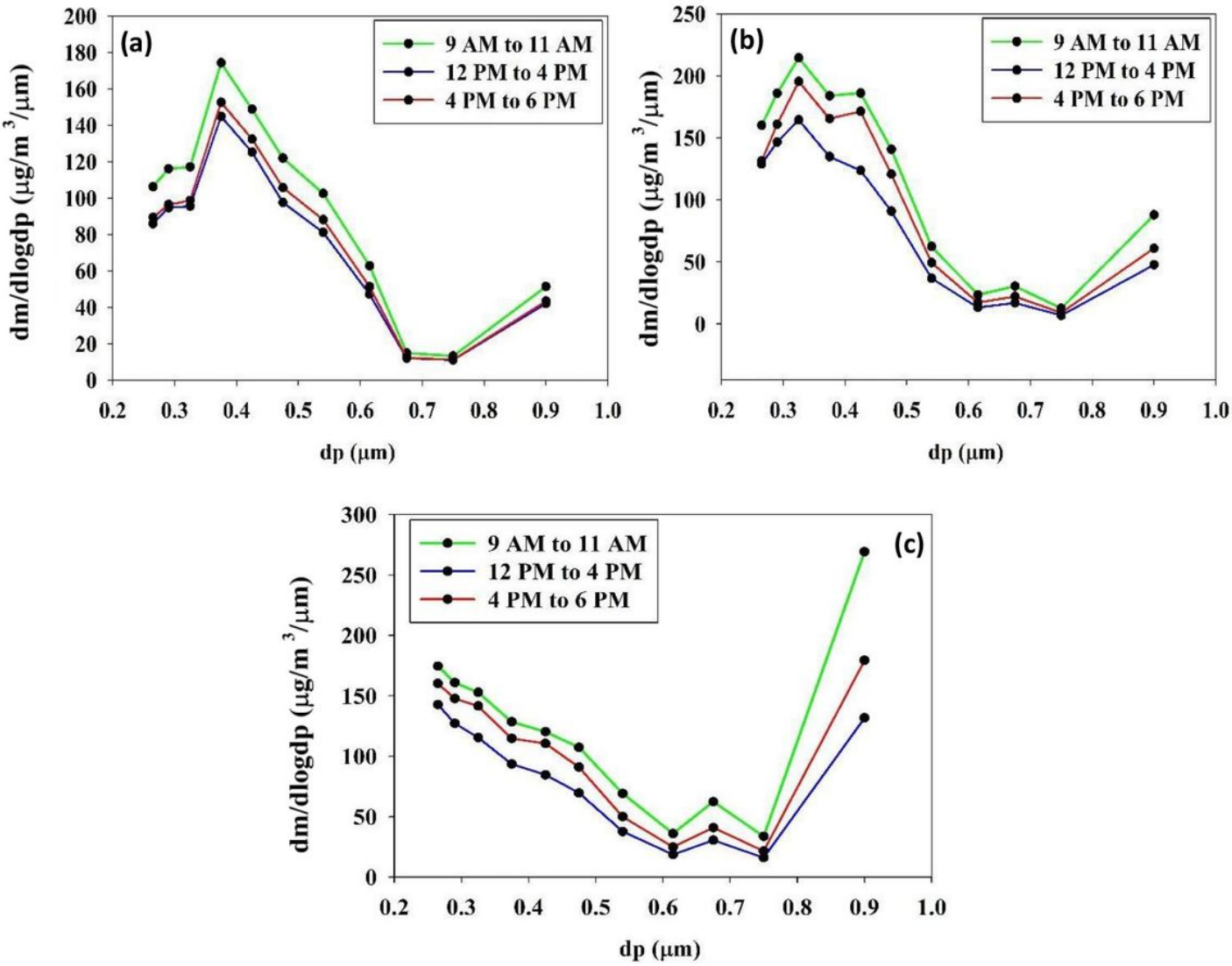

Figure 2

Lognormal mass size distribution of fine particulate matter at different locations a. HP, b. YP-Gate, and c. Sakinaka

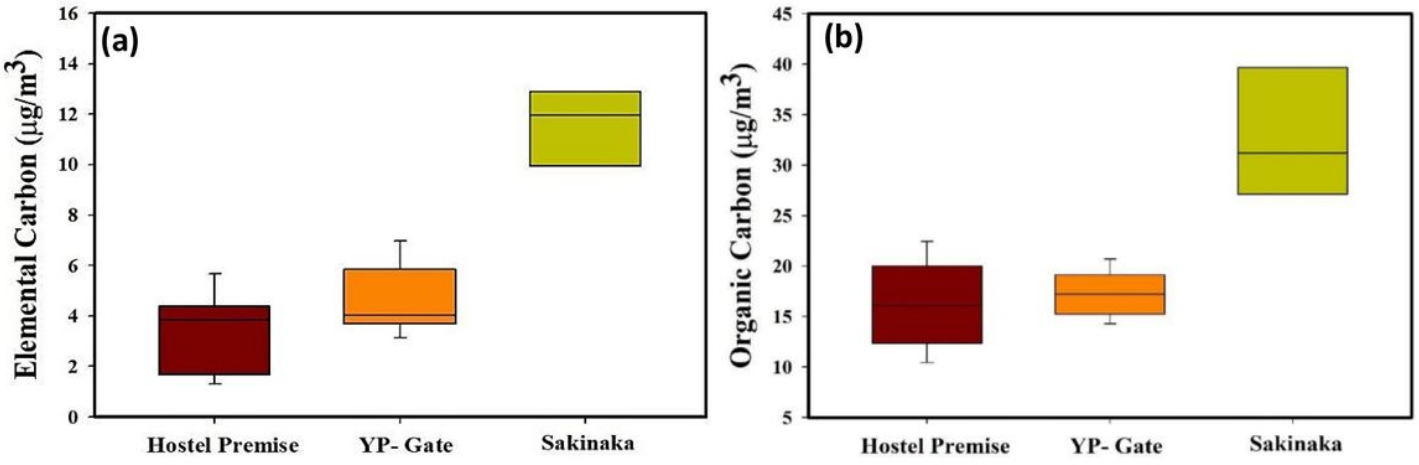

Figure 3

Average concentration of the (a) Elemental carbon and (b) Organic carbon at the study locations, HP, YP-Gate, and Sakinaka

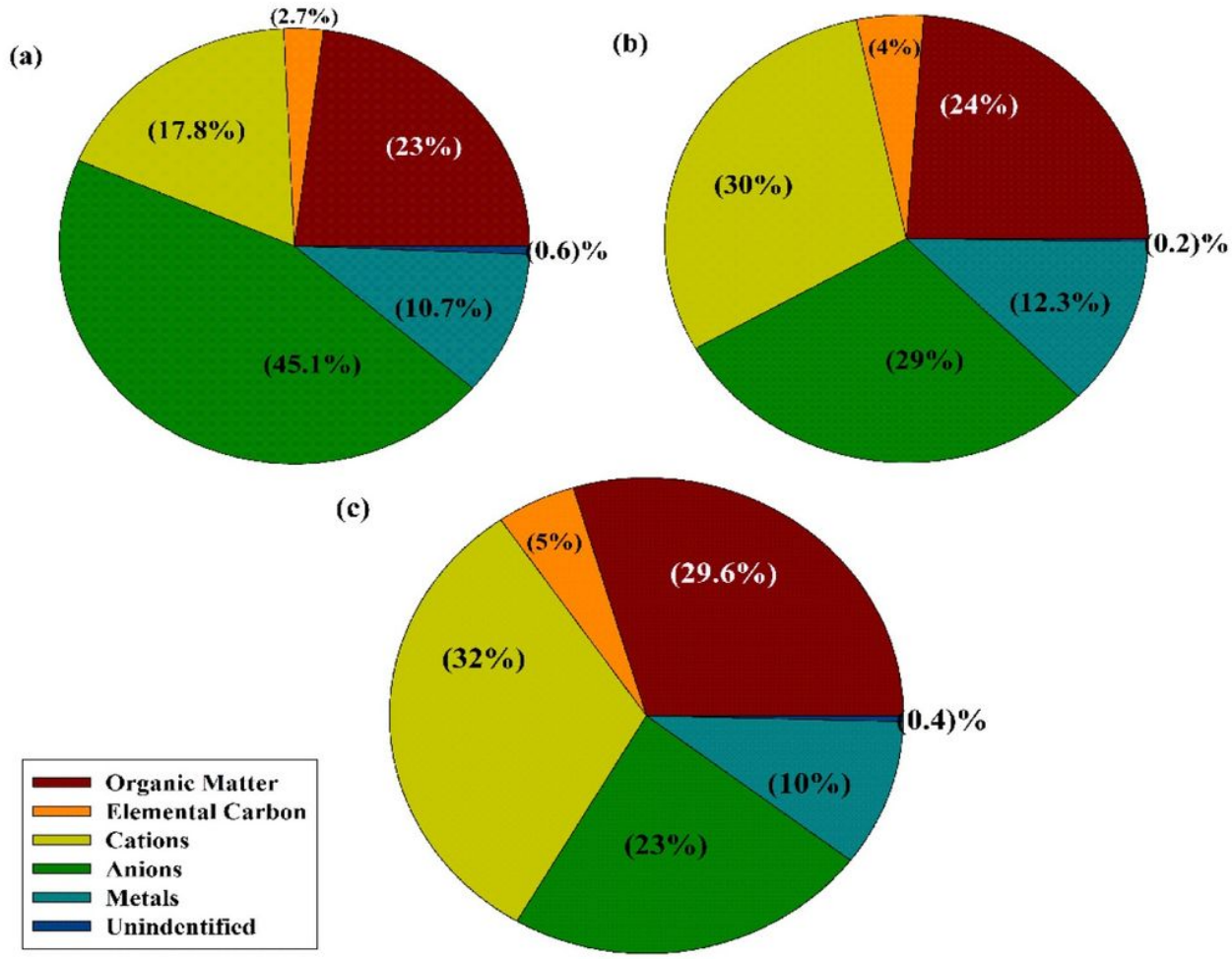

Figure 4

The $PM_{2.5}$ chemical characterization at different locations in Mumbai, a. HP, b. YP-Gate and, c. Sakinaka Junction.

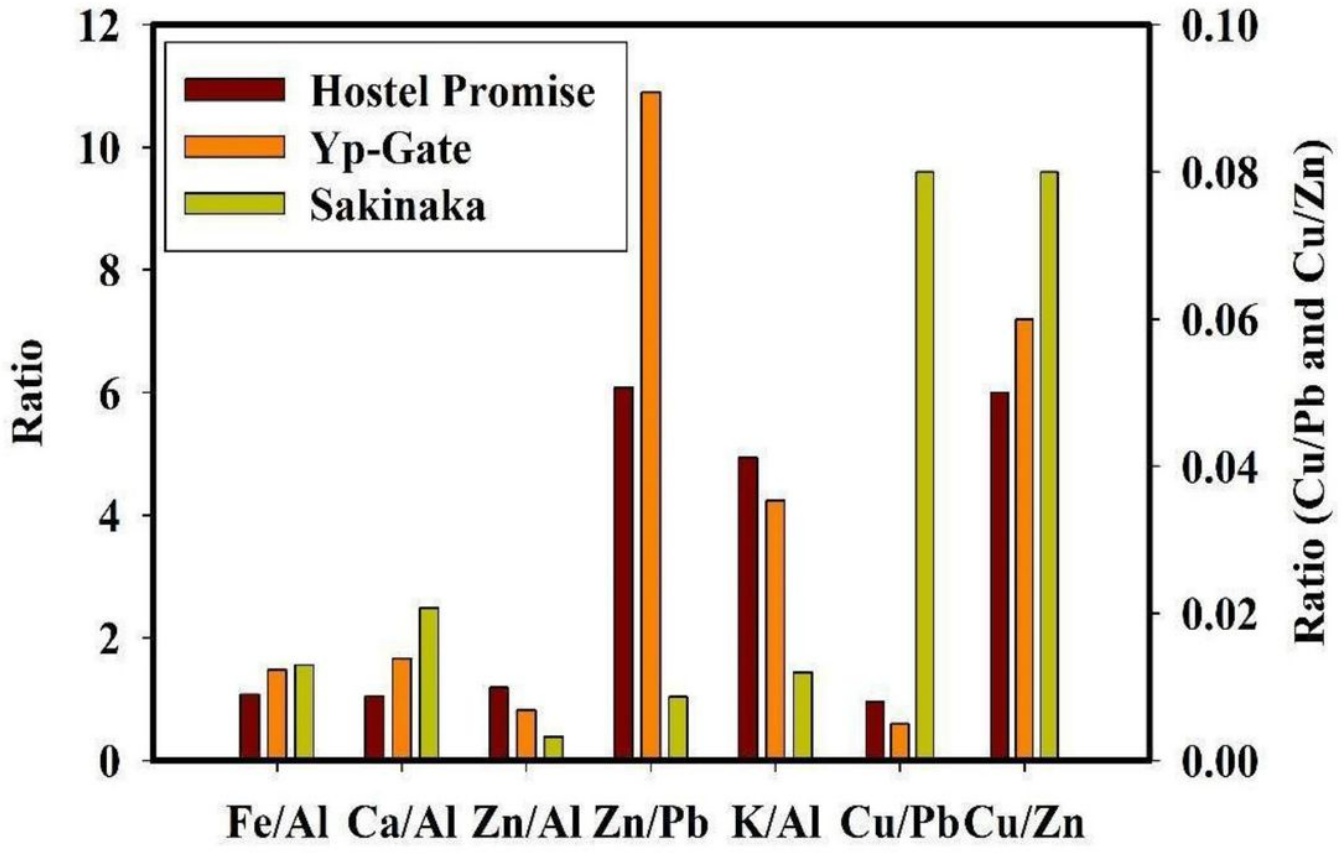

Figure 5

Elemental ratios at different sites (Left axis for Cu/Pb and Cu/Zn ratio)

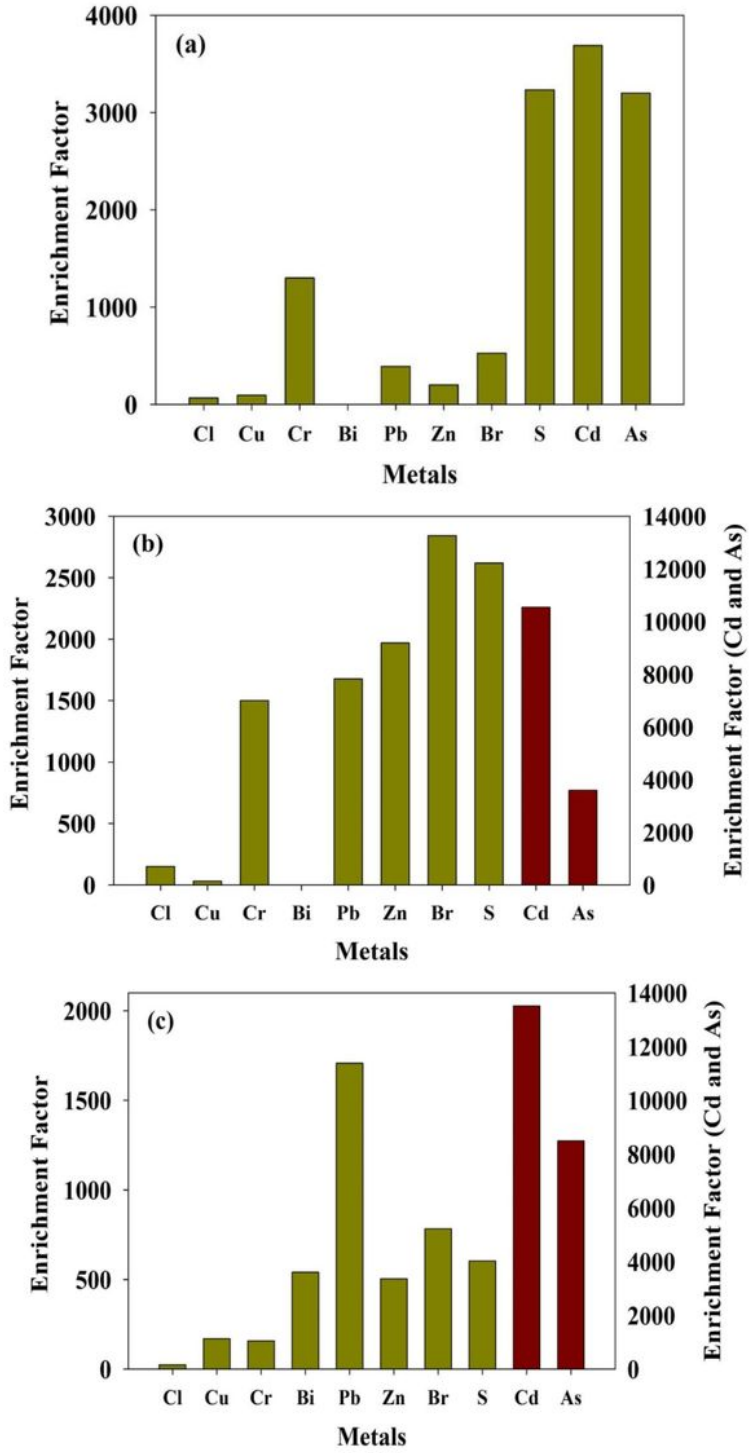

Figure 6

Enrichment factor of metals in $PM_{2.5}$ at a. HP, b. YP-Gate, and c. Sakinaka (For YP-Gate and Sakinaka, two scales are used for high value.

Supplementary Files

This is a list of supplementary files associated with this preprint. Click to download.

- SupplementaryJAC.docx